Supporting Information

Precision Surface Modification of Solid Oxide Fuel Cells via Layer-by-Layer Surface Sol-Gel Deposition

Nicholas Kane, Yucun Zhou, Weilin Zhang, Yong Ding, Zheyu Luo, Xueyu Hu, and Meilin Liu[*]

The amount of catalyst was also estimated through analysis of the STEM images (see **Figure S1**). After firing, the particles on the 15-PrO_x-LSCF closely match a spherical cap. Using the estimated surface coverage also from STEM analysis, the volume of the spherical cap, and the average size of these caps, the mass of catalyst per area can be estimated. The inset in Figure S1 shows the idealization of a single catalyst particle on the surface of the LSCF, which has a volume of V_i as shown in equation 1.

$$V_i = \frac{\pi h}{6}(3a^2 + h^2) \quad [1]$$

The fraction of surface coverage as calculated by top down STEM images, f_c, can be related to the area of a single cap, the number of caps n, and the total area A.

$$Af_c = \pi a^2 n \quad [2]$$

The total volume of catalyst V_c is simply the number of caps by the volume of each cap V_i. Combining equation 1 and 2 in equation 3 gives equation 4.

$$V_c = nV_i \quad [3]$$

$$V_c = \frac{Af_c h}{6a^2}(3a^2 + h^2) \quad [4]$$

Considering the density of the catalyst ρ, the mass normalized by area is shown in equation 5.

$$\frac{m}{A} = \frac{\rho f_c h}{6a^2}(3a^2 + h^2) \quad [5]$$

From STEM images, the average of a and h are 7.5 nm and 5 nm, respectively. ρ for Pr_6O_{11} is 6.5 g cm^{-3} and f_c is 0.23 for 15-PrO_x-LSCF. Thus, the total mass change over 15 cycles is estimated to be 429 ng cm^{-2}, or 28.6 ng cm^{-2} per cycle. This value is about one third the value estimated by QCM. One source of error is the relatively small area evaluated from STEM images. While the surface modification is quite uniform over the whole electrode, this introduces uncertainty. The assumption that all particles are identical and of a standard size also introduces error into this estimation. Finally, the coated QCM sensor was not fired, thus there may be minor mass loss during the firing process, possibly reducing the mass as any remaining $Pr(O^iPr)_3$ is oxidized.

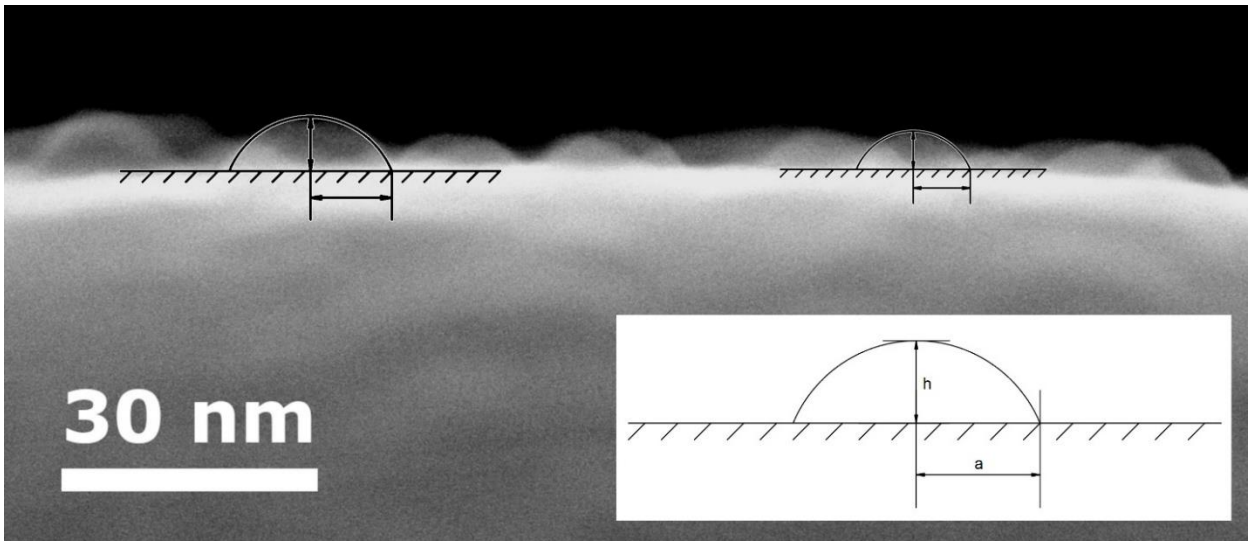

Figure S1. STEM image of the surface of 15-PrO_x-LSCF showing the approximation of the surface particles as spherical caps. The inset shows a diagram of the spherical cap.

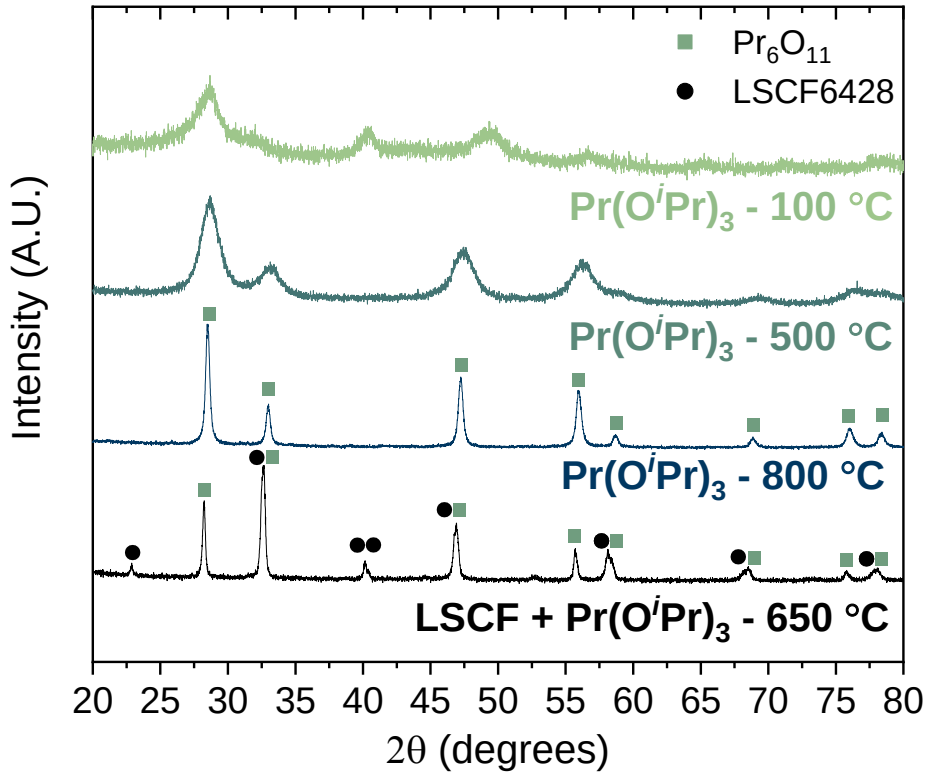

Figure S2. X-ray diffractograms of praseodymium isopropoxide with and without LSCF reacted with water after annealing at various temperatures.

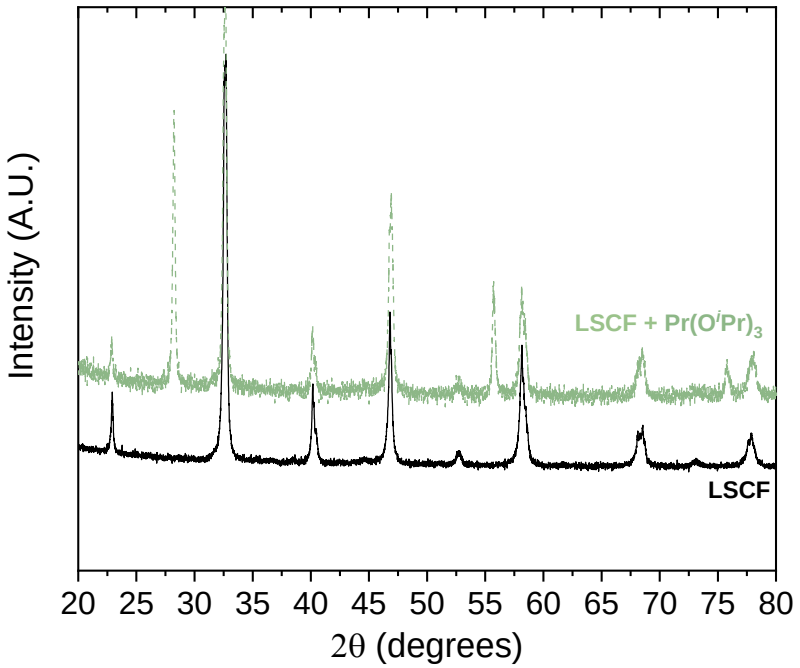

Figure S3. XRD diffractograms comparing the LSCF fired with $Pr(O^iPr)_3$ at 650 °C for 10 hours to the unmodified commercial LSCF powder. The LSCF peak positions show no significant differences.

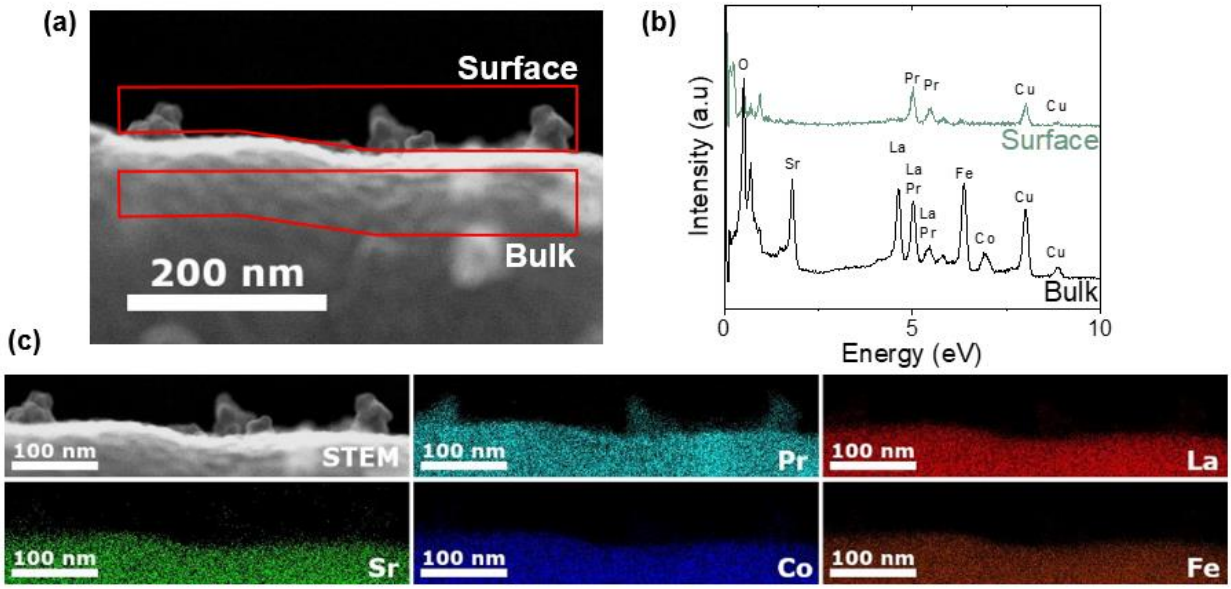

Figure S4. STEM EDX characterization of 45-PrO_x-LSCF. (a) STEM image of 45-PrO_x-LSCF, highlighting the scan location of the bulk and surface spectra. (b) EDX spectra of the surface particles and bulk 45-PrO_x-LSCF. (c) EDX mapping of the same location on 45-PrO_x-LSCF showing the presence of Pr containing particles on the surface of the LSCF.

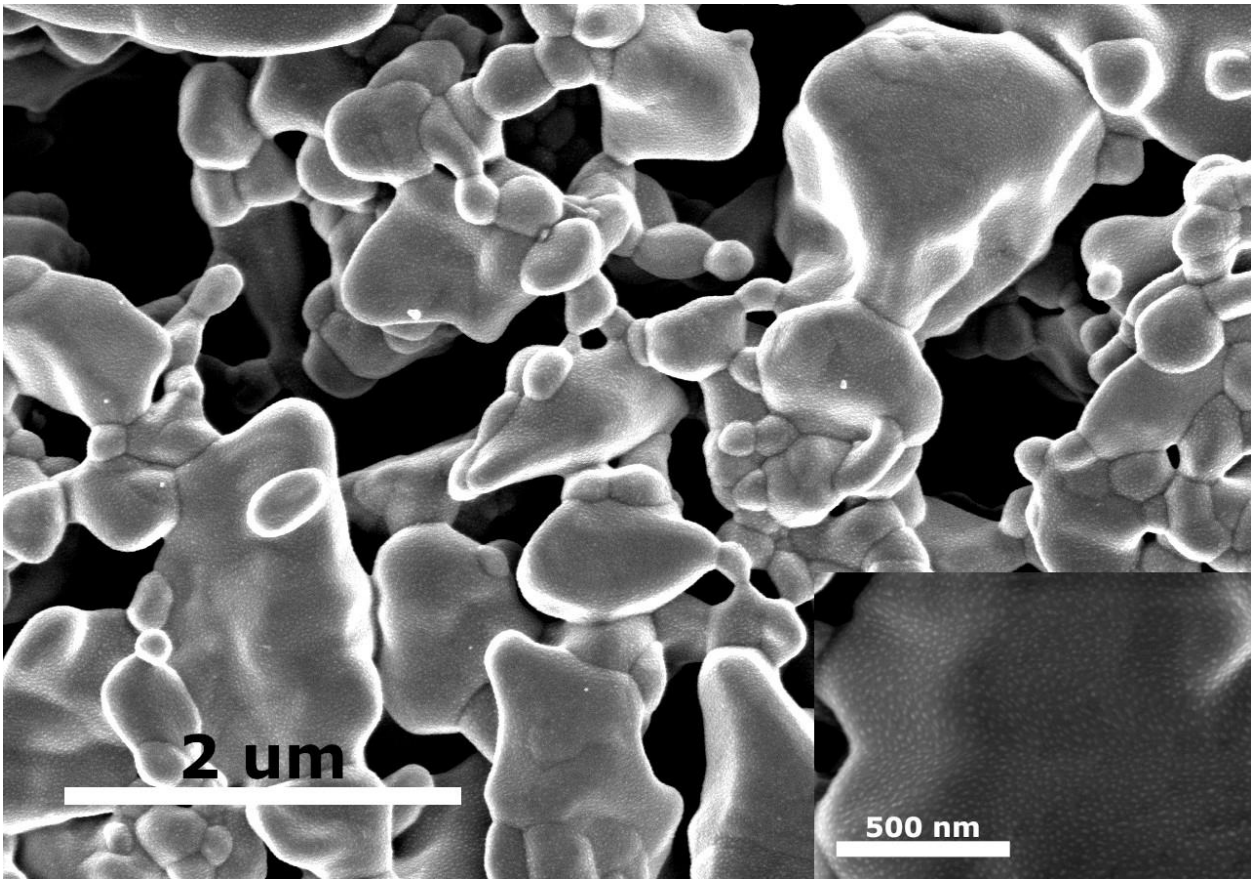

Figure S5. SEM images of the cross section of a 15-PrO_x-LSCF electrode after firing at 650 °C for 2 hours showing the uniformity of the surface modification over a large area. The high resolution inset details the surface particles present on the entirety of the electrode shown in the low magnification image.

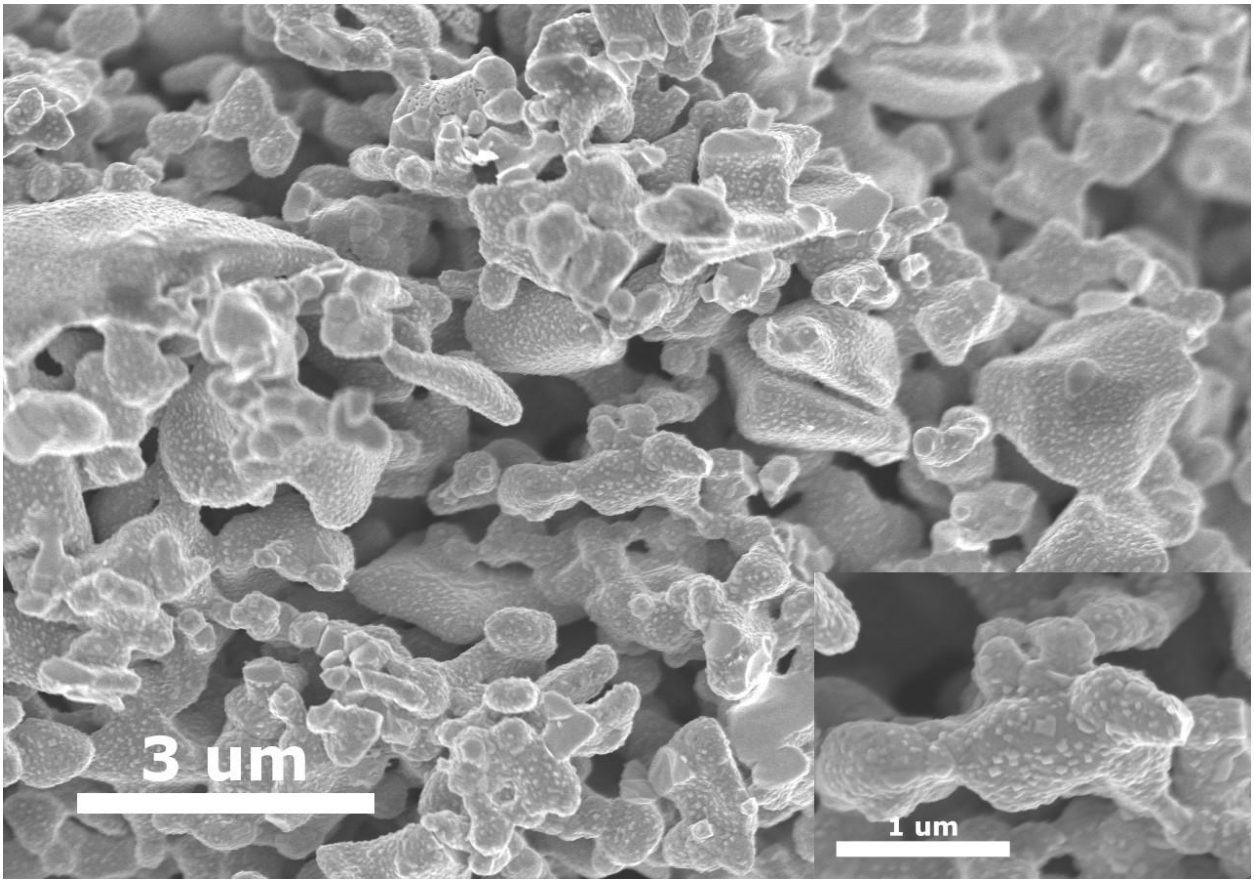

Figure S6. SEM images of the cross section of a 45-PrO_x-LSCF electrode after stability testing 650 °C for over 200 hours showing the uniformity of the surface modification over a large area. The high resolution inset details the surface particles present on the entirety of the electrode shown in the low magnification image.

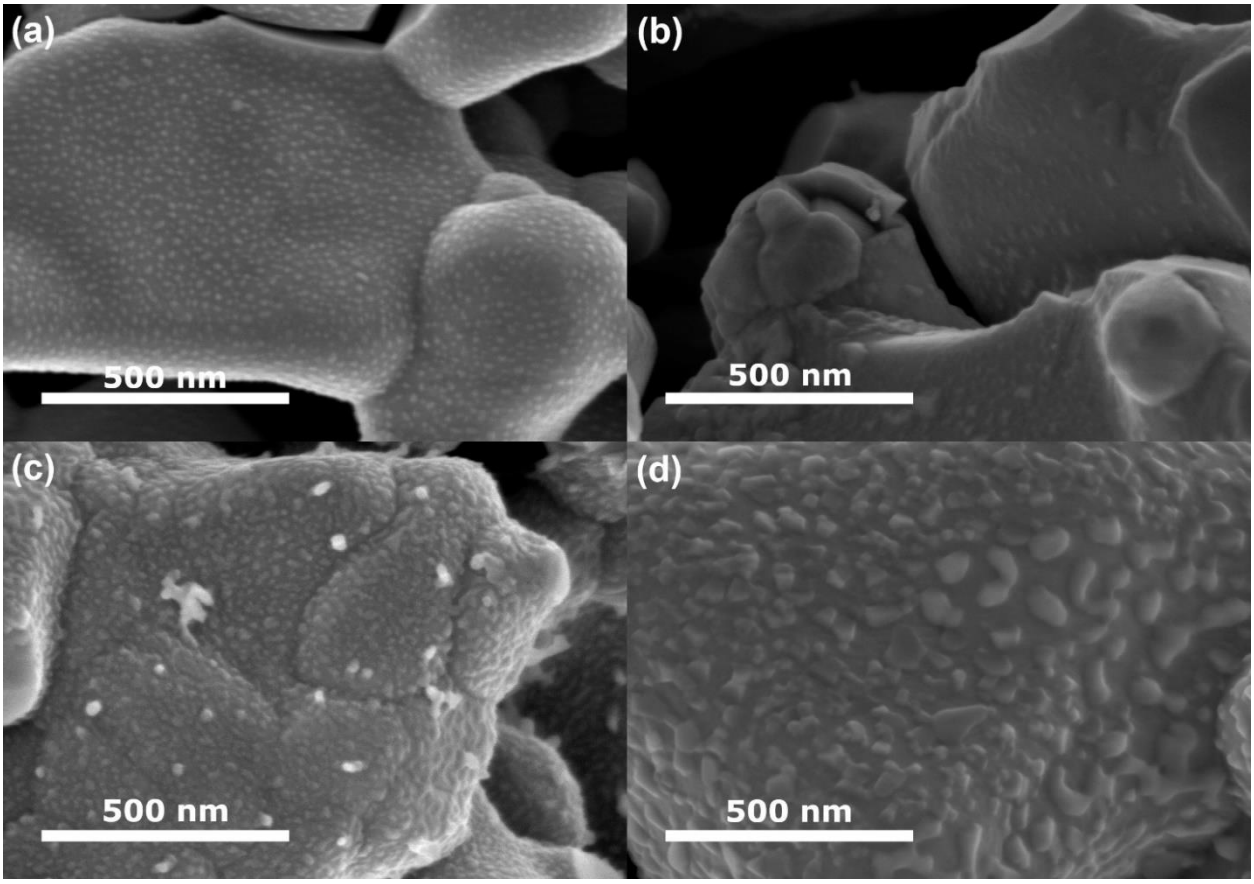

Figure S7. SEM images of the cross section of 15-PrO_x-LSCF and 45-PrO_x-LSCF electrodes after firing at 650°C for 2 hours and after the 200 hour stability test at 650°C showing the coarsening of the PrO_x surface modification. (a) 15-PrO_x-LSCF before and (b) after 200 hours. (c) 45-PrO_x-LSCF before and (d) after 200 hours.

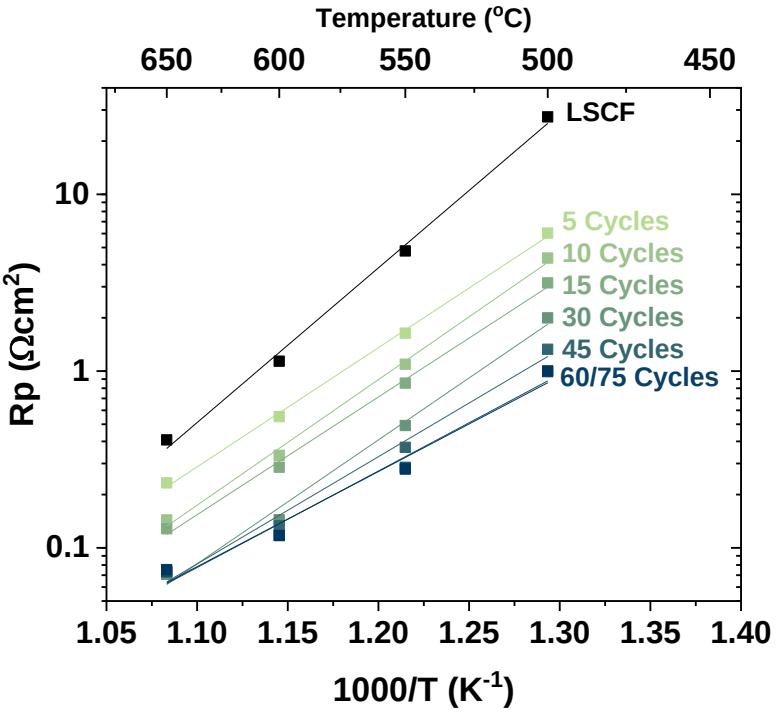

Figure S8. Activation energy plot of PrO_x-modified LSCF symmetrical cells with various cycle counts from 5 to 75 cycles at 0 hours.

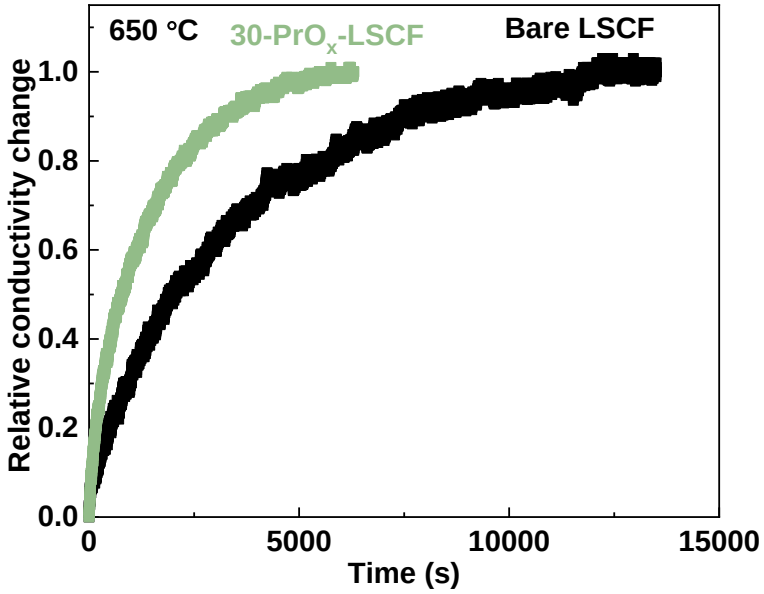

Figure S9. Relative conductivity as a function of time after switching atmospheres during the ECR measurement.

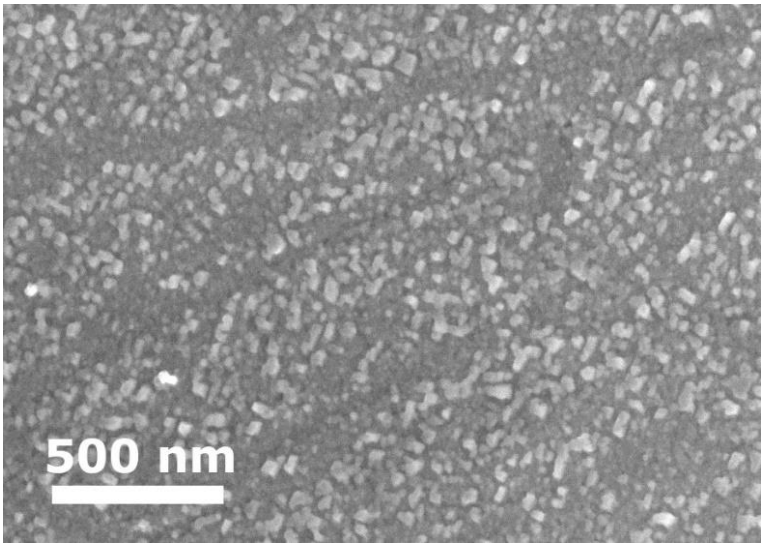

Figure S10. SEM image of the surface of the 30-PrO_x-LSCF bar sample for ECR measurement.

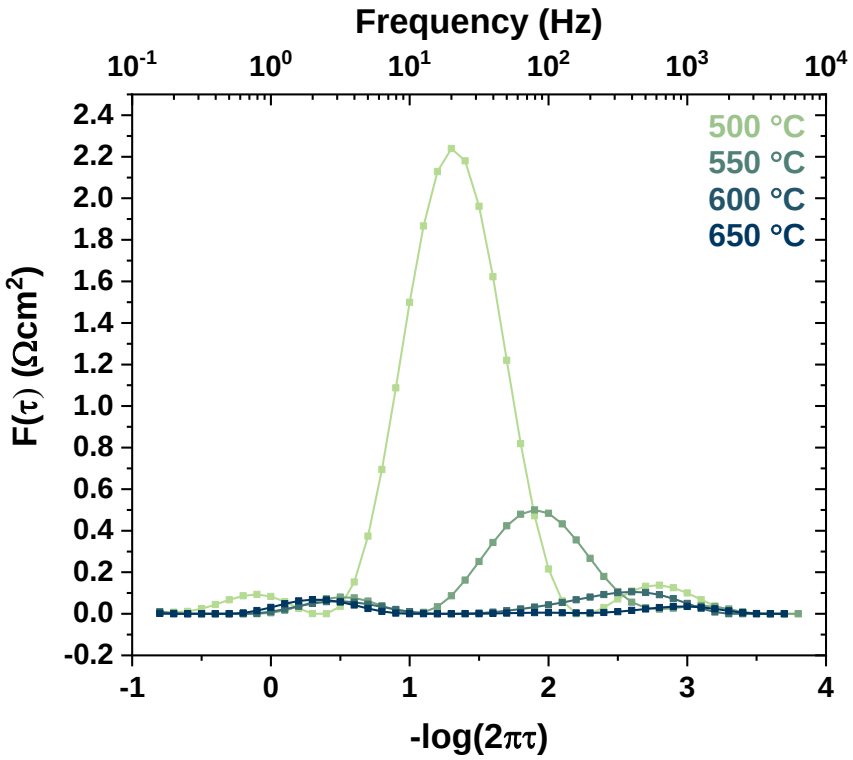

Figure S11. Distribution of relaxation times for 30-PrO_x-LSCF at various temperatures from 500 °C to 650 °C.

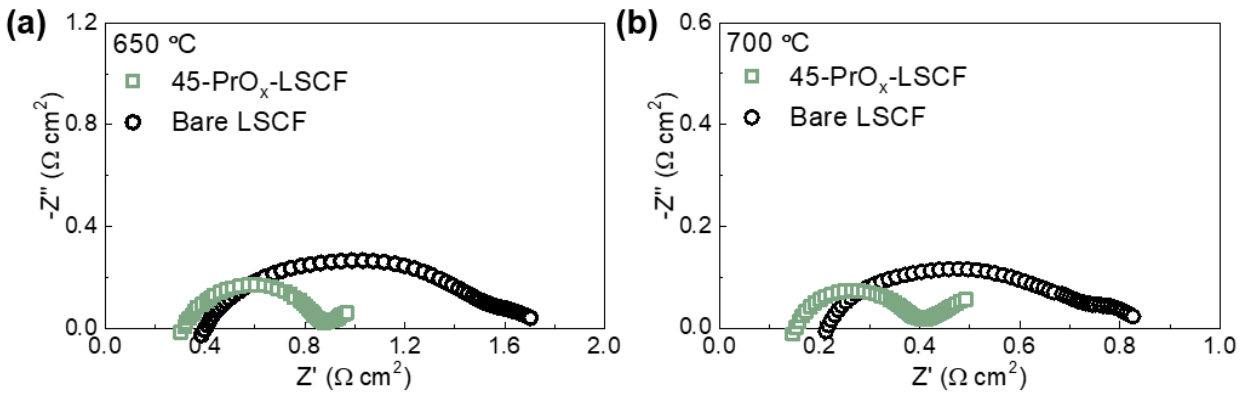

Figure S12. Nyquist plots of YSZ-based single cells with bare LSCF and 45-PrO$_x$-LSCF cathodes at (a) 650 °C and (b) 700 °C.

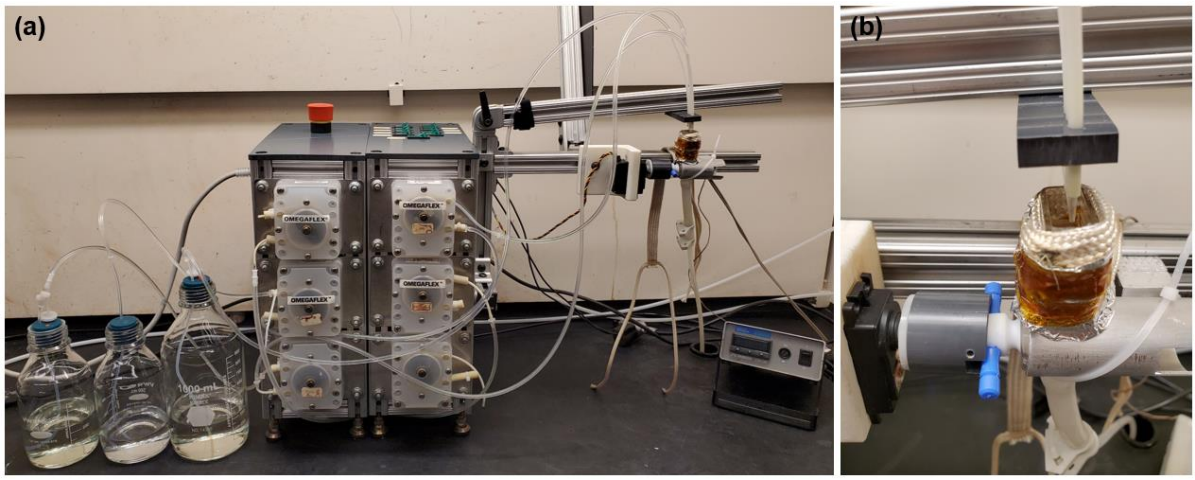

Figure S13. Images of (a) the surface sol-gel system, showing the precursor solutions, computer control box with peristaltic pumps, and (b) heated reaction chamber. Not pictured is a vacuum pump with a liquid waste trap.